

1

## 2 Effective connectivity of LSD-induced ego dissolution

3

4 Devon Stoliker<sup>1\*</sup>, Leonardo Novelli<sup>1</sup>, Franz X. Vollenweider<sup>3</sup>, Gary F. Egan<sup>1,2</sup>, Katrin H. Preller<sup>3+</sup>,  
5 and Adeel Razi<sup>1,2,4,5+</sup>

6 <sup>1</sup>Turner Institute for Brain and Mental Health, Monash University, Clayton, VIC

7 <sup>2</sup> Monash Biomedical Imaging, Monash University, Clayton, VIC

8 <sup>3</sup> Department of Psychiatry, Psychotherapy & Psychosomatics, University Hospital for  
9 Psychiatry, Zurich, Switzerland

10 <sup>4</sup> Wellcome Centre for Human Neuroimaging, UCL, London, United Kingdom

11 <sup>5</sup>CIFAR Azrieli Global Scholars Program, CIFAR, Toronto, Canada

12

13

14 + Joint Senior Authors

15 \* Corresponding author

16 Name: Devon Stoliker

17 Address: Monash Biomedical Imaging,

18 762-772 Blackburn Rd,

19 Clayton VIC 3168. Australia.

20 Email: [devon.stoliker@monash.edu](mailto:devon.stoliker@monash.edu)

21

22 Keywords: Ego dissolution; LSD; resting state functional MRI; dynamic causal modelling;

23 predictive coding

24

25

26 **Abstract:**

27

28 Classic psychedelic-induced ego dissolution involves a shift in the sense of self and blurring of boundary  
29 between the self and the world. A similar phenomenon is identified in psychopathology and is associated  
30 to the balance of anticorrelated activity between the default mode network (DMN) –  
31 which directs attention inwards – and the salience network (SN) – which recruits the dorsal attention  
32 network (DAN) to direct attention outward. To test whether change in anticorrelated networks underlie  
33 the peak effects of LSD, we applied dynamic causal modeling to infer effective connectivity of resting  
34 state functional MRI scans from a study of 25 healthy adults who were administered 100mg of LSD, or  
35 placebo. We found that change in inhibitory effective connectivity from the SN to DMN became  
36 excitatory, and inhibitory effective connectivity from DMN to DAN decreased under the peak effect of  
37 LSD. These changes in connectivity reflect diminution of the anticorrelation between resting state  
38 networks that may be a key neural mechanism of LSD-induced ego dissolution. Our findings suggest the  
39 hierarchically organised balance of resting state networks is a central feature in the construct of self.  
40

41 **Significance:**

42  
43 The findings can inform the parallel between the maintenance of subject-object boundary and changes to  
44 anticorrelated canonical resting state brain networks. Effective connectivity informs the hierarchical  
45 organisation of brain networks underlying modes of perception. Moreover, the anticorrelation of brain  
46 networks is an important measure of mental function. Understanding the neural mechanisms of  
47 anticorrelation change under psychedelics help identify its relationship to psychosis and its association to  
48 psychedelic assisted therapeutic outcomes.

49

50 Keywords – fMRI, psychedelics, resting state connectivity, Dynamic causal modelling, LSD, ego dissolution

51

52 **Introduction:**

53

54 Classic psychedelics are powerful substances with low toxicity that can temporarily alter brain activity  
55 and produce profound changes to consciousness (Carhart-Harris, 2018; Johnson, Richards, & Griffiths,  
56 2008; Preller & Vollenweider, 2018; F. X. Vollenweider, 1998; F. X. Vollenweider et al., 1997).  
57 Historical use of their mind altering effects that are undergoing translation into modern clinical therapies  
58 may constitute a crucial component of their therapeutic efficacy (Roseman, Nutt, & Carhart-Harris, 2018;  
59 Yaden & Griffiths, 2020). The subjective effects of classic psychedelics are characterised by *ego*  
60 *dissolution* (Preller & Vollenweider, 2018; Stoliker, Egan, Friston, & Razi, 2021), described as the shift  
61 in the sense of self and a loss of boundary between the subjective and the objective world (Dittrich, 1998;  
62 Studerus, Gamma, & Vollenweider, 2010; Vollenweider and Smallridge, 2021; Grof, 1980; Lebedev et  
63 al., 2015). Ego dissolution is a validated construct (Dittrich, 1998; Matthew M. Nour, Evans, Nutt, &  
64 Carhart-Harris, 2016; Studerus et al., 2010) and is thought to involve changes to resting state network  
65 (RSN) activity (Müller, Dolder, Schmidt, Liechti, & Borgwardt, 2018; Preller et al., 2018; Stoliker et al.,  
66 2021).

67  
68 Functional magnetic resonance imaging (fMRI) investigations indicate activity across the brain is  
69 functionally integrated and forms multiple RSNs (Raichle, 2015). RSNs are associated to mental activity  
70 and the balance of connectivity between them is associated to the direction of conscious attention  
71 (Michael D. Fox et al., 2005; K. J. Friston, 2011; Greicius & Menon, 2004). The default mode network  
72 (DMN) composed of the medial prefrontal cortex (mPFC), posterior cingulate cortex (PCC), and  
73 (bilateral) angular gyrus (AG) is a RSN that activates primarily in the absence of immediate external goal-  
74 directed attention (Raichle et al., 2001). Its function in self-focused thinking and attention suggests its  
75 close relationship to the ego (Andrews-Hanna, Smallwood, & Spreng, 2014). In contrast, the dorsal  
76 attention network (DAN) is a RSN activated during external-focused task-driven attention (Corbetta &  
77 Shulman, 2002; Michael D. Fox & Raichle, 2007) and is usually considered to be composed of the frontal  
78 eye field (FEF) and intraparietal sulcus (IPS) bilaterally. The activity of the DMN and DAN are identified  
79 as anticorrelated and predictably alternate with the inward or outward switching of attention (Michael D.

80 Fox et al., 2005). The DMN-DAN anticorrelation can be hypothesised to be a mechanism maintaining the  
81 boundary between the subject (observer) and object (observation) that is altered during experiences of  
82 psychedelic ego dissolution.

83

84 A third resting state network, the salience network (SN), acts as the switching mechanism coordinating  
85 the direction of attention between internal and external stimuli (Liang et al., 2015; Seeley et al., 2007).  
86 The SN's cardinal regions are the dorsal anterior cingulate cortex (dACC) and anterior insula (AI). Both  
87 the dACC and AI are consistently coactivated across cognitive tasks (Swick, Ashley, & Turken, 2011),  
88 however the dACC is more involved in response selection and conflict monitoring (Ide, Shenoy, Yu, &  
89 Li, 2013; Menon, 2011) while the AI receives greater multimodal sensory input (Averbeck & Seo, 2008)  
90 (Vogt & Pandya, 1987), detects behaviourally relevant stimuli (Menon, 2015) and coordinates the  
91 dynamic interactions of anticorrelated networks (Menon & Uddin, 2010; Sridharan, Levitin, & Menon,  
92 2008).

93

94 Coordinated interactions between these networks produce important biopsychological functions. SN  
95 coactivation with the DAN detects bottom-up features in the visual environment that are infrequent or  
96 biologically significant (Egner et al., 2008; Fecteau & Munoz, 2006; Szczepanski, Pinski, Douglas,  
97 Kastner, & Saalmann, 2013) and also enables the detection of resources relevant to higher-order goals  
98 (Menon, 2015). Furthermore, anticorrelated function between the SN and DMN is a biomarker of  
99 efficient cognition (Chand, Wu, Hajjar, & Qiu, 2017; Putcha, Ross, Cronin-Golomb, Janes, & Stern,  
100 2016). Trauma to the white matter tracts within the SN that connect the rAI and dACC predicts  
101 dysregulated DMN function (Bonnelle et al., 2012). Importantly, abnormality of SN connectivity and its  
102 anticorrelated interactions is indicative of schizophrenia (Manoliu et al., 2014), psychosis (Palaniyappan  
103 & Liddle, 2012; Wotruba et al., 2013) and internalizing disorders (Peterson, Thome, Frewen, & Lanius,  
104 2014) (See Menon 2015 for review of SN associations to psychopathology) (Menon, 2011).

105

106 The DMN and SN have been previously investigated in relation to unique senses of self. The SN has been  
107 suggested to be involved in an aspect of the self defined as the basic sense of being rooted within a body,  
108 termed the *minimal* or *embodied* self (Blanke & Metzinger, 2009; Lebedev et al., 2015; Legrand & Ruby,  
109 2009). This association is supported by changes to the SN documented in psychopathology (Liu et al.,  
110 2018), meditation (Doll, Hölzel, Boucard, Wohlschläger, & Sorg, 2015; Ramirez Barrantes et al., 2019)  
111 and psychedelic-induced ego dissolution (Lebedev et al., 2015) (see Supplementary Table 1 for a subset  
112 of psychedelic findings related to networks and regions of interest). The pre-reflective qualities that  
113 define the minimal self have also been suggested as antecedents of the *narrative* aspect of self (Ho,  
114 Preller, & Lenggenhager, 2020; M. M. Nour & Carhart-Harris, 2017). The narrative aspect of self is  
115 believed to be under the control of the DMN and describes self-related mental activity and personal  
116 identity (Metzinger, 2003; Millière, 2017) that strongly parallels the classic Freudian construct of ego  
117 (Carhart-Harris & Friston, 2010; Cieri & Esposito, 2019). These parallels have led to exploratory  
118 investigations of the DMN under psychedelic-induced ego dissolution that indicate a general pattern of  
119 reduced connectivity (Carhart-Harris & Friston, 2010; Cieri & Esposito, 2019; Ruban & Kolodziej, 2018;  
120 Franz X. Vollenweider & Preller, 2020).

121  
122 Reduced DMN activity has also been identified in meditation and is a feature of improved mental health  
123 (Batchelor, 2008; Judson A. Brewer et al., 2011; Hasenkamp, Wilson-Mendenhall, Duncan, & Barsalou,  
124 2012; Millière, Carhart-Harris, Roseman, Trautwein, & Berkovich-Ohana, 2018). Psychedelics have been  
125 reported to reduce symptoms of patients experiencing internalising mental health disorders (Carhart-  
126 Harris et al., 2018; Nutt & Carhart-Harris, 2020; Ruban & Kolodziej, 2018). Altered self-boundaries may  
127 be important to these therapeutic outcomes (Griffiths et al., 2016; Roseman et al., 2018; Ross et al.,  
128 2016). Nascent alignment between the free energy principle and psychoanalytic processes proposes that  
129 high-order, secondary processes of the ego function to minimise free energy of lower-orders (Cieri &  
130 Esposito, 2019; Karl Friston, 2009; K. Friston, Kilner, & Harrison, 2006; Herzog et al., 2020).  
131 Psychedelic-induced free energy increase in networks such as the DMN is suggested to disinhibit high

132 order inhibitory selection of bottom-up channels and enable consideration of alternate hypotheses  
133 underlying making sense of the world (Carhart-Harris & Friston, 2019; Safron, 2021; Stoliker et al.,  
134 2021). These mechanisms may broadly account for experiences of ego dissolution (Stoliker, Egan, &  
135 Razi, 2021). An early interpretation of psychedelics noted in *filtration theory* similarly suggests  
136 improvements follow psychedelic reduction of ego-protective defenses (Connolly, 2018; Freud, 1894;  
137 Stoliker et al., 2021; Swanson, 2018). Understanding network changes in ego dissolution may inform how  
138 network interactions relate to clinical outcomes. Meditation is also recognised for its benefits to wellbeing  
139 and resembles a similar trajectory of ego disarmament by seeking cessation of the self (Batchelor, 2008;  
140 Millière et al., 2018). The practice of meditation has demonstrated clinical utility (Goyal et al., 2014) and  
141 can enhance wellbeing by altering the relationship between self and other (Dambrun, 2017). Pertinently, a  
142 form of meditation termed *nondual awareness* meditation reduces the anticorrelation of extrinsic and  
143 intrinsic activated brain regions and produces a subjective experience of dissolving subject-object  
144 boundaries (Josipovic, Dinstein, Weber, & Heeger, 2012). These findings indicate anticorrelation under  
145 control of the SN as a neural mechanism that underlies ego dissolution.

146  
147 Anticorrelation between the DMN and task positive networks under psilocybin has previously been  
148 investigated with the findings demonstrating reduced anticorrelation when participants experienced ego  
149 dissolution, under psilocybin (intravenous infusion, 2mg dissolved in 10ml) (Carhart-Harris et al., 2012).  
150 However, a similar investigation, under ayahuasca (oral brew, 2.2. mL/kg body weight, containing 0.8  
151 mg/ml DMT and 0.21 mg/ml harmine) failed to identify anticorrelation changes (Palhano-Fontes et al.,  
152 2015). The inability of functional connectivity analyses to determine the direction of connectivity  
153 between networks in these studies suggests the value of adopting mechanistic approaches to determine  
154 changes in effective connectivity of networks under psychedelics. Dynamic Causal Modeling (DCM) is a  
155 Bayesian method of inference based on task based or resting state fMRI time series activity of brain  
156 regions (K. J. Friston, Harrison, & Penny, 2003; Karl J. Friston, Kahan, Biswal, & Razi, 2014). DCM can  
157 disentangle hierarchical RSN and regional interactions by determination of the directionality of

158 connectivity. DCM has been previously applied to investigate thalamic connectivity to the cortex under  
159 LSD (Preller et al., 2019) that indicated the SN is at the apex of the DMN and DAN triple network  
160 hierarchy (Zhou et al., 2018). The SN's position in this hierarchy and its mediating role to control the  
161 switching of DAN and DMN activity suggests that change to the SN by psychedelics may influence their  
162 patterns of anticorrelated activity. The SN and DMN share associations to aspects of self and the  
163 importance of their connectivity in psychopathology suggests change in their connectivity may be a  
164 mechanism of ego dissolution that underlies a shift in the sense of self (Northoff et al., 2006; Scalabrini et  
165 al., 2020).

166

167 Therefore, to understand the neural mechanisms of ego dissolution and inform the biological basis of the  
168 subject-object relationship, the directed changes to these networks under the classic psychedelic lysergic  
169 acid diethylamide (LSD) was investigated. LSD effects were examined across placebo (two weeks apart  
170 from LSD administration), peak effects at 75 minutes and later effects at 300 minutes post LSD  
171 administration using DCM analysis to reveal regional and network connectivity changes. Ego dissolution  
172 (quantified as oceanic boundlessness (OBN)) was measured on the five dimensions of altered states of  
173 consciousness scale (5D-ASC) (Studerus et al., 2010). Based on previous research that associated the  
174 networks under investigation to self and subject-object boundaries, we hypothesised the association  
175 between effective connectivity would change during the peak effects of LSD and ego dissolution. DMN-  
176 DAN was tested for change to subject-object boundaries and SN-DMN was tested for change to the self.  
177 However, the direction of excitatory-inhibitory connectivity change remained exploratory. Additionally,  
178 we measured connectivity of regions composing the networks of interest and the (hierarchical)  
179 connectivity strength between networks.

180

181 **Results:**

182

183 **Acute Drug Effects**

184

185 *Functional connectivity changes*

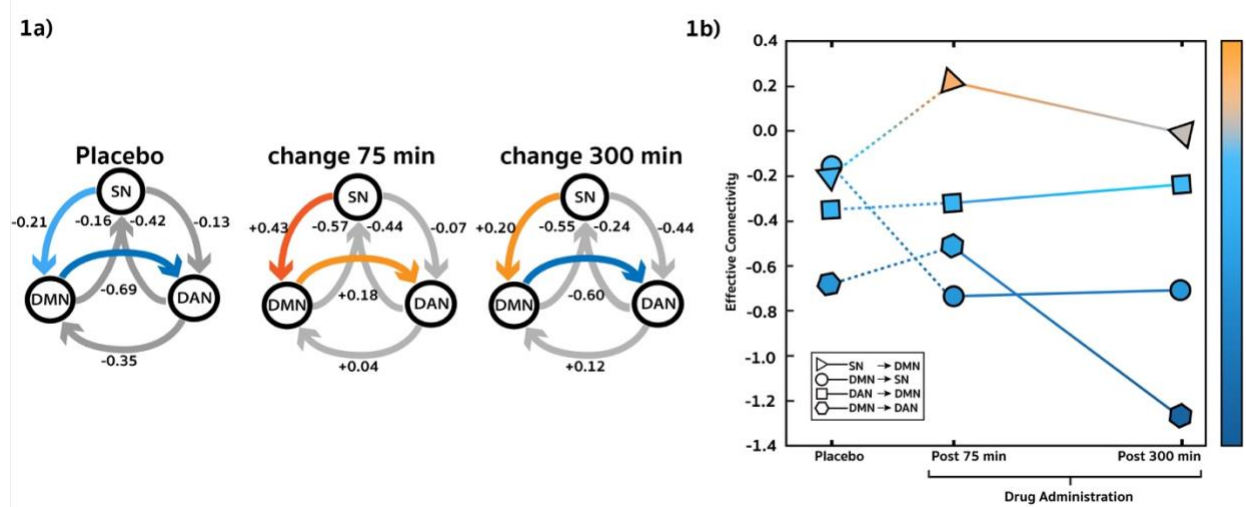
186 Functional connectivity across groups demonstrated a fading of the pattern of anticorrelation between  
187 DMN and DAN and SN, from placebo to peak effects of LSD before showing evidence of restoration in  
188 the later effects at 300 minutes. Group level regional functional connectivity matrix across each condition  
189 (placebo, 75 minutes after LSD administration and 300 minutes post LSD administration) is provided in  
190 Supplementary Fig. 1.

191

192 *Between networks changes in effective connectivity*

193 The first resting-state fMRI scan was done 75 minutes post administration of LSD which is during the  
194 peak effects of LSD. The connectivity strength between networks was computed as the difference  
195 between averaged and unsigned efferent and afferent connection parameters between networks (see  
196 methods for further details) (Zhou et al., 2018). As shown in Fig. 1a), at this time, group level, between  
197 networks, effective connectivity increased from the SN to DMN causing the directed connection to  
198 become excitatory. A similar change was observed in the excitatory connectivity from the DMN to the  
199 DAN resulting in reduced inhibitory connectivity (see Fig. 1c). SN to DMN and DMN to DAN changes  
200 from placebo are greatest during the peak effects at 75 minutes and reduce in the later effects at 300  
201 minutes (see Fig. 1a) and 1b). These changes show reduced hierarchical connectivity strength (i.e.,  
202 increased afferent connections) of the SN and increased hierarchical connectivity strength (i.e., increased  
203 efferent connections) of the DMN and DAN from placebo (SN= -1.16 Hz, DMN = + 0.32 Hz, DAN =

204 +0.41 Hz, see Supplementary S4 for explanation and quantitative analysis).



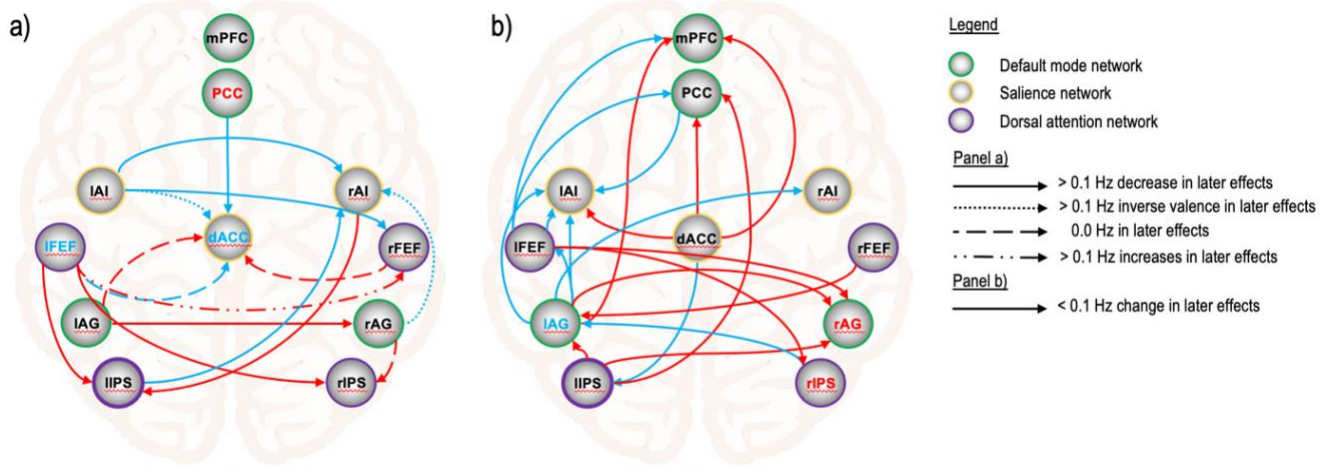
205

206 Fig 1. Network effective connectivity change under peak effects of LSD. a) Highlighted connections show  
207 changes in effective connectivity compared to placebo signifying peak effect. b) Network effective  
208 connectivity change graphed across placebo, peak effects and later effects. Same data as a) and b) but  
209 plotted as a line graph for better visualization. Values display effect sizes (posterior expectations) of  
210 connections in Hz. All results are for posterior probability > 0.99.

211

212 Between regions changes in effective connectivity.

213 Between regions effective connectivity that underly the SN to DMN changes include increased inhibitory  
214 self-connectivity of the dACC and lFEF and effective connectivity from the lAG to rAG, lFEF to the lIPS,  
215 lIPS to rAI. These regions are highlighted because the change in their effective connectivity show large  
216 effect sizes during the peak effects than in later effects of LSD. Moreover, lAI to dACC and rAG to rAI  
217 effective connectivity show large effect size change from inhibitory in the peak effects of LSD to excitatory  
218 in the later effects (see Fig. 2, panel a) below and Supplementary Fig. 3 for untranslated effective  
219 connectivity matrices across conditions).



220

221 Fig 2. Region effective connectivity signifying a) peak and b) lasting effects of LSD. Red lines and lettering  
222 indicate excitatory change; blue lines and lettering indicate inhibitory change. Only connections with  
223 change from placebo to 75 minutes post LSD > 0.1 Hz are included. Panel a) illustrates effective  
224 connectivity with change > 0.1 Hz from peak effects at 75 minutes to the later effects at 300 minutes,  
225 signifying connectivity unique to the peak effects of LSD. See Supplementary Table 2 for posterior  
226 expectations (effect sizes) and credible intervals. Panel b) illustrates effective connectivity with change <  
227 0.1 Hz from peak effects at 75 minutes to the later effects at 300 minutes, signifying connectivity  
228 changes that last over the effects of LSD. See Supplementary Table 3 for posterior expectations (effect  
229 size) and credible intervals. All results are for posterior probability > 0.99.

230

### 231 Lasting effects

232 Between networks changes in effective connectivity.

233 LSD effects are also distinguished by changes from placebo that last across time under LSD. Increased  
234 DAN to DMN and decreased DMN to SN effective connectivity at 75 minutes remains evident 300 minutes  
235 after LSD (see Fig. 1, panel a) above, and see Supplementary Fig. 3 for effect size and posterior  
236 probabilities).

237

238 *Between regions changes in effective connectivity.*

239 Effects lasting across time under LSD are identified by change in lAG and rIPS self-inhibition, lFEF to  
240 mPFC inhibition and lIPS to PCC excitation. These connections show large effect sizes from placebo to  
241 peak effect that remain to the later effects of LSD (see Fig. 2, panel b) above and Supplementary Fig. 3 for  
242 untranslated effective connectivity matrices across conditions).

243  
244 The results demonstrate increased effective connectivity of the DMN to DAN and SN to the DMN during  
245 the peak effects of LSD. These changes correspond with reduced SN hierarchical connectivity strength (i.e.,  
246 increased afferent connections) and coincide with a fading of the functional anticorrelation (see  
247 Supplementary Fig. 1 for functional connectivity results).

248

## 249 **Discussion:**

250  
251 This investigation seeks to understand how effective connectivity between antcorrelated large-scale brain  
252 networks is related to ego dissolution. Our analysis reveals between network effective connectivity changes  
253 that occur with a diminution of the pattern of antcorrelation under the peak effects of LSD. Bidirectional  
254 changes in effective connectivity between the DMN and DAN were investigated for their relationship to  
255 subject-object boundaries. We identified reduced inhibition of the DMN to the DAN under the peak effects  
256 of LSD. The reduced inhibition is largely lost in the later effects, when ego dissolution dissipates. This  
257 indicates reduced inhibition of the DMN to DAN as a feature of peak LSD effects that may relate to the  
258 fading of the functional antcorrelation between the two networks. Reduced DMN to DAN inhibition may  
259 also represent an increased transmission and connection of the narrative self to the sense of object.  
260 Moreover, hierarchical organisation and strength of networks were calculated using efferent vs afferent  
261 connections (Zhou et al., 2018). The DMN and DAN showed increased hierarchical connectivity strength  
262 during the peak effects of LSD and segregate from SN, under the peak effects of LSD (See Supplementary

263 S4). The increase in hierarchical connectivity strength of the DMN and DAN reinforces evidence of their  
264 fading anticorrelation that may contribute to the dissolution of the boundary between the subject and the  
265 object. The opposite effective connectivity from DAN to DMN also displays reduced inhibition under LSD.  
266 However, this change remains over the course of time suggesting it is not a primary mechanism of the  
267 reduced functional anticorrelation between them or ego dissolution.

268

269 Network level DMN-DAN changes are supported by the lAG to rAG connectivity. The AG serves  
270 functions in autobiographical memory and bodily awareness (Bréchet, Grivaz, Gauthier, & Blanke, 2018).  
271 AG also operates complex language functions and makes meaning out of visually perceived self-related  
272 words (Yaoi, Osaka, & Osaka, 2015). Excitatory change in the connection from lAG to rAG in placebo to  
273 the peak effects of LSD is greater than in the later effects suggesting the importance of this connection in  
274 the peak effects.

275

276 Inclusion of the SN in this analysis enabled measurement of its effective connectivity to the DMN and  
277 DAN under LSD. The change to the coordinated balance of networks, under the control of SN, by LSD  
278 may be an important but overlooked neural mechanism of ego dissolution suggested by the superiority of  
279 SN in this hierarchy of triple networks (Zhou et al., 2018). Previous reports of reduced anticorrelation  
280 (Carhart-Harris et al., 2012), reduced SN integrity (Lebedev et al., 2015) in occurrences of ego  
281 dissolution, and its hypothesised function in basic conscious-awareness also indicate the value of  
282 measuring SN connectivity in the anticorrelation between DMN and DAN. Moreover, ego dissolution has  
283 previously been suggested to involve the breakdown of sub-personal processes underlying the minimal  
284 self, a suggestion that is consistent with Bayesian models of phenomenal selfhood in which the subjective  
285 structure of conscious experience is determined from the optimisation of prediction in perception and  
286 action (Clark, 2013; Karl Friston, 2010; Millière, 2017). The change in the SN effective connectivity  
287 under the peak effects of LSD is our most pronounced finding. SN connectivity to the DMN changes  
288 from inhibitory to excitatory before returning to inhibitory in the later effects. This flip of valence

289 suggests SN connectivity change to the DMN is mechanistic in the peak effects of LSD and may  
290 indirectly influence the DMN-DAN interactions. The opposite connection, the DMN to SN, shows an  
291 inverse pattern of change from placebo, suggesting reduced DMN influence over the SN which lasts over  
292 time. The SN to DMN connectivity change may therefore be a more likely mechanism of ego dissolution  
293 representing a quietening of narrative self in the peak effects of LSD that reduces in the later effects. This  
294 change in DMN function to minimise free energy and suppress prediction errors that in Freudian terms  
295 may liberate the ego from the reality principle (Carhart-Harris & Friston, 2010; Cieri & Esposito, 2019). SN to  
296 DMN change is accompanied by reduced hierarchical connectivity strength of the SN that is characterised  
297 by increased SN afferent connections and increased DMN efferent connections. The SN has previously  
298 been identified to be hierarchically superior to the DMN and DAN (Zhou et al., 2018). We demonstrate  
299 the divergence of SN and DMN hierarchical strength under the peak effects of LSD shift the hierarchical  
300 order of the SN beneath the DMN.

301  
302 The changes to region level effective connectivity underlying the SN are demonstrated by dACC self-  
303 connectivity under the peak effects of LSD. The dACC is a central brain hub involved in cognitive  
304 functions, social emotions (Andrews-Hanna et al., 2014; Etkin, Egner, & Kalisch, 2011; Preller et al., 2015)  
305 and performance monitoring (Ham et al., 2014) and has previously been noted in social cognition under  
306 psilocybin (Preller et al., 2016). Enlargement of the ACC has also been reported after regular use of  
307 ayahuasca (Carlos Bouso et al., 2015). We find dACC self-connectivity inhibition and inhibitory  
308 connectivity from the IAI to the dACC under the peak effects of LSD, compared to placebo. In the later  
309 effects dACC inhibition become less inhibitory while the IAI changes to excitatory. The AI is involved in  
310 interoceptive awareness (Chong, Ng, Lee, & Zhou, 2017) and the shift of internal and external perception  
311 (Menon & Uddin, 2010; Sridharan et al., 2008). Damage to SN connectivity predicts dysregulated DMN  
312 function (Menon, 2011) and alteration of SN anticorrelated interactions share association with psychosis  
313 and internalising disorders (Bonnelle et al., 2012). dACC and IAI inhibition at the peak effects of LSD may  
314 indicate the role of SN inhibition that is relevant to ego dissolution and psychedelic assisted therapy.

315 Connectivity between the DMN and SN is also noted in region changes from the rAG to rAI. This  
316 connection follows the lAI to dACC pattern of inhibition in the peak effects and excitation in the later  
317 effects, suggesting a reduced influence of the DMN to the SN during peak effects, when ego dissolution  
318 occurs that may suggest a shifting sense of self.

319

320 The PCC and dACC represent cardinal regions of the DMN and SN respectively and are related to the  
321 narrative and minimal aspects of self (Lebedev et al., 2015; Millière, 2017). The connectivity changes  
322 between them are reported in association to meditation and the mindfulness capacities of meditators (Judson  
323 A. Brewer et al., 2011; Millière et al., 2018; Palhano-Fontes et al., 2015). We provided evidence of the  
324 excitation from the dACC to PCC in our effective connectivity analysis under peak effects (see  
325 Supplementary Fig. 3), which may suggest dACC cognitive control functions influence on self-related  
326 functions of PCC. Interestingly, self-connectivity of the PCC, a hub region of DMN, increases excitation  
327 during the peak effects of LSD. PCC involvement in self-awareness is well documented (J. A. Brewer,  
328 Garrison, & Whitfield-Gabrieli, 2013; Northoff et al., 2006) and activity of this region is commonly  
329 observed to decrease under psychedelics (see Supplementary Table 1).

330

331 Other notable regions in our analysis include the FEF and IPS. The FEF operates visual attention  
332 (Thompson, Biscoe, & Sato, 2005) and the IPS serves functions directing attention and memory (Corbetta  
333 & Shulman, 2002; Michael D. Fox, Corbetta, Snyder, Vincent, & Raichle, 2006). The nearby right inferior  
334 parietal lobule (rIPL) is also associated with the sense of agency and self-other discrimination (Chaminade  
335 & Decety, 2002; Lucina Q. Uddin, Molnar-Szakacs, Zaidel, & Iacoboni, 2006). Smaller effect sizes  
336 involving these regions were identified in our analysis (see Supplementary Fig. 3) suggesting more subtle  
337 widespread brain changes occur under the effects of LSD.

338

339 Taken together, under the peak effects of LSD, a strong increase in change of effective connectivity, and a  
340 widening of gap between the hierarchical connectivity strength of the SN vs the DMN and DAN shifts in

341 a direction antithetical to normal hierarchical organisation. This may be said to resemble a collapse – or  
342 flattening – of the hierarchy, during peak effects of LSD, when ego dissolution occurs (See Fig. 1 and  
343 Supplementary S4). Effective connectivity explains this effect as increased excitatory connectivity from  
344 the SN to the DMN. These directed connection changes and the hierarchical strength changes may  
345 function to alter the relationship between the minimal and narrative senses of self. The direction of this  
346 change suggests the influence of the minimal-self traverses over the narrative-self and may relate to the  
347 shift in sense of self described under ego dissolution.

348

349 Modelling the connectivity of ego dissolution can provide a means to determine the neural mechanisms that  
350 underlie the perception of inner and outer reality. The present research establishes important steps to  
351 identify the change in network interactions associated with the dichotomy of the subject-object relationship  
352 under LSD. The networks involved in this interaction are important in cognitive function and mental  
353 wellbeing, suggesting that understanding their change due to psychedelics may elucidate mechanisms of  
354 psychedelic clinical therapy. Consideration of practical and theoretical challenges may aid future research  
355 directed to study ego dissolution and the anticorrelation between brain networks.

356

357 Our relatively small sample size (n=20) is clearly a limitation. Sample size and processing pipeline strongly  
358 impact the reliability of results. Small sample size may also account for unexpected placebo effective  
359 connectivity in our group of subjects. A second practical limitation is the large variance of participant  
360 subjective responses to a standard dose of LSD (100mg). Averaging the connectivity of participants  
361 experiencing highly variable subjective shifts in consciousness may dilute the effective connectivity  
362 representing LSD's subjective effects. An alternative to increased sample size may be predetermining  
363 participant dose-response and including only participants with high subjective responses in the analysis.  
364 Replicating the investigation of anticorrelated networks with alternate classic psychedelic substances  
365 including psilocybin, ayahuasca and mescaline in addition to LSD will be a worthy direction to validate our  
366 results. Furthermore, comparisons with similar altered forms of consciousness reporting ego change such

367 as psychosis and meditation may also help discern the function of components in the anticorrelated  
368 networks.

369

370 The selection of regions and region coordinates composing the networks of interest require careful attention.  
371 For example, some studies define the DAN as composed by the posterior prefrontal cortex, the inferior  
372 precentral sulcus, the superior occipital gyrus, the middle temporal motion complex, and the superior  
373 parietal lobule (Andrews-Hanna et al., 2014). Similarly, the DMN may be composed using the inferior  
374 parietal lobule (Di & Biswal, 2014) closely situated to the IPS used in the DAN in this analysis. The  
375 composition of regions composing networks can strongly impact results. Furthermore, selection of region  
376 centroids can also affect the results. Previous work using this LSD data set used different coordinates for  
377 the PCC and identified its increased self-inhibition (Preller et al., 2019), although our analysis identified  
378 decreased PCC inhibition. Avoiding this problem is challenging due to anatomical variability between  
379 participants, variability in the method of determining coordinates and the selection of regions composing  
380 networks. However, the standardisation of these considerations across studies is important to improve the  
381 accuracy and reliability of findings across studies.

382

383 Future work to extend the current scope of analysis to include connectivity dynamics of additional task  
384 positive networks anticorrelated to the DMN and under control of the SN is required. For example, non-  
385 psychedelic research involving the CEN (central executive network, also known as the frontoparietal central  
386 executive network (FPCEN)) has been conducted to investigate schizophrenia (Leptourgos et al., 2020;  
387 Menon, 2011), meditation (Doll et al., 2015) and control of attention (Corbetta & Shulman, 2002). Its  
388 importance is further signified by investigations of large-scale network interactions and anticorrelations  
389 with the DMN (Andrews-Hanna et al., 2014; Bolton et al., 2020; Menon, 2018). Inclusion of the CEN in  
390 anticorrelation investigations may provide a more complete account of anticorrelated network changes  
391 associated to ego dissolution.

392

393 Theoretical challenges include consensus on the nature and situation of ego dissolution within the taxonomy  
394 of psychedelic-induced effects. Psychometric investigations of psychoanalytic based concepts of ego-  
395 functions and measurement of their brain connectivity are recommended future directions. Psychedelics  
396 may contribute to these investigations by altering and allowing measurement of brain mechanisms  
397 hypothesised to underlie psychoanalytic constructs. Integration of psychoanalytic theory and brain  
398 connectivity processes may be important to identifying processes involved in enabling the sense of self and  
399 experiences of ego dissolution.

400

#### 401 **Conclusions:**

402

403 The between network balance of anticorrelated activity of specific RSNs depends on subtle adjustments to  
404 network activation. Mental wellbeing and efficient cognition rely on the balance of these interactions. LSD  
405 appears to shift the balance of network activation and diminish the anticorrelation between brain networks  
406 responsible for internal and external modes of perception. Observed increases in effective connectivity from  
407 the DMN to DAN and increased hierachal strength of these networks under peak effects may account for  
408 the blurring of boundary between subject and object experienced in ego dissolution. Ego dissolution also  
409 involves a shift in the sense of self that may be explained by changes to the interactions between SN and  
410 DMN. These networks are related to distinct aspects of self. Increased effective connectivity from the SN  
411 to the DMN and decreased SN hierarchical connectivity strength emphasise hierarchical flattening and  
412 increased salience functions reaching the DMN under the peak effects of LSD. Future research could model  
413 how changes to these networks effective connectivity may support psychedelic therapeutic outcomes. The  
414 neuroscientific study of psychedelic-induced ego dissolution reminds us that constructs and representations  
415 of self and internal and external reality exist in connectivity dynamics. This intriguing understanding may  
416 inspire future investigations of sentience and consciousness to learn how normal brain function mechanisms  
417 contribute to the subject-object relationship and frame our perspective of reality.

418

419 **Methods:**

420

421 *Participants*

422 The data analysed in this paper were collected as part of a larger study (registered at ClinicalTrials.gov  
423 (NCT02451072)), which is reported in (Preller et al., 2017) and (Preller et al., 2018), and was approved by  
424 the Cantonal Ethics Committee of Zurich. 25 subjects (19 males and 6 females; mean age = 25.24 y; SD =  
425 3.72 y; range = 20–34 y) were recruited through advertisements at universities in Zurich, Switzerland. All  
426 participants were deemed healthy after screening for medical history, physical examination, blood analysis,  
427 and electrocardiography. The Mini-International Neuropsychiatric Interview (MINI-SCID), the Diagnostic  
428 and Statistical Manual of Mental Disorders, fourth edition self-rating questionnaire for Axis-II personality  
429 disorders (SCID-II), and the Hopkins Symptom Checklist (SCL-90-R) were used to exclude subjects with  
430 present or previous psychiatric disorders or a history of major psychiatric disorders in first-degree relatives.  
431 Participants were asked to abstain from prescription and illicit drug use two weeks prior to first testing and  
432 throughout the duration of the study, and abstain from alcohol use 24 hours prior to testing days. Urine tests  
433 were also used to exclude pregnancy. Further exclusion criteria included left-handedness, poor knowledge  
434 of the German language, cardiovascular disease, history of head injury or neurological disorder, history of  
435 alcohol or illicit drug dependence, MRI exclusion criteria, including claustrophobia, and previous  
436 significant adverse reactions to a hallucinogenic drug. All participants provided written informed consent  
437 statements in accordance with the declaration of Helsinki before participation in the study. Subjects  
438 received written and oral descriptions of the study procedures, as well as details regarding the effects and  
439 possible risks of drug treatment.

440

441 *Design*

442 A double blind, randomized, placebo-controlled, cross-over study was performed. Testing days occurred  
443 two weeks apart and participants were orally administered either LSD after pretreatment with 179 mg

444 Mannitol and 1 mg Aerosil (LSD condition) or 179 mg Mannitol and 1 mg Aerosil after pre-treatment with  
445 179 mg Mannitol and 1 mg Aerosil (placebo condition). Resting state scans (10 minutes each) were taken  
446 75 and 300 minutes following administration.

447

448 *MRI Data Acquisition and Preprocessing*

449 MRI data were acquired on a Philips Achieva 3.0T whole-body scanner. A 32-channel receive head coil  
450 and MultiTransmit parallel radio frequency transmission was used. Images were acquired using a whole-  
451 brain gradient-echo planar imaging (EPI) sequence (repetition time, 2,500 ms; echo time, 27 ms; slice  
452 thickness, 3 mm; 45 axial slices; no slice gap; field of view,  $240 \times 240 \text{ mm}^2$ ; in-plane resolution,  $3 \times 3 \text{ mm}$ ;  
453 sensitivity-encoding reduction factor, 2.0). Additionally, high-resolution anatomical images (voxel size,  $0.7$   
454  $\times 0.7 \times 0.7 \text{ mm}^3$ ) were acquired using a standard T1-weighted 3D magnetization prepared rapid-acquisition  
455 gradient echo sequence. The acquired images were analysed using SPM12 (<https://www.fil.ion.ucl.ac.uk>).  
456 The pre-processing steps of the images consisted of slice-timing correction, realignment, spatial  
457 normalization to the standard EPI template of the Montreal Neurological Institute (MNI), and spatial  
458 smoothing using a Gaussian kernel of 6-mm full-width at half maximum. Head motion was investigated  
459 for any excessive movement, but movement did not exceed 3 mm in any participant.

460

461 *Extraction of region coordinates across subjects*

462 Group ICA for fMRI Toolbox (GIFT, <http://mialab.mrn.org/software/gift>) (Calhoun et al. 2001) was used  
463 to identify the three resting state networks of interest from placebo scans. Pre-processed resting state fMRI  
464 data were spatially sorted into 20 components (Biswal et al. 2010; Shirer et al. 2012; Tsvetanov et al. 2016)  
465 and spatially matched with pre-existing network templates (Shirer et al. 2012).

466 Networks were composed of cardinal regions constituting a core part of DMN (Andrews-Hanna, Reidler,  
467 Sepulcre, Poulin, & Buckner, 2010; Dixon et al., 2017) which reliably show anticorrelation with the DAN  
468 and SN (Chen, Glover, Greicius, & Chang, 2017; Dixon et al., 2017; M. D. Fox, Zhang, Snyder, &  
469 Raichle, 2009; Fransson, 2005; L. Q. Uddin, Kelly, Biswal, Castellanos, & Milham, 2009) and followed

470 the selection of regions in a related investigation by Zhou and colleagues (Zhou et al., 2018).  
471 Identification of cardinal nodes within each intrinsic network – averaged across our subjects – was  
472 located using peak RSN activity of clusters within networks ( $p=.05$ ) visualized using xjView toolbox  
473 (<https://www.alivelearn.net/xjview>). Associations between peak coordinates and cardinal nodes of  
474 network regions of interest (ROI) were determined by expert visual inspection. The MNI coordinates of  
475 the selected ROIs are listed in Table 4.  
476 A generalized linear model (GLM) was used to regress 6 head motion parameters (3 translation and 3  
477 rotational), white matter and cerebrospinal fluid signals from preprocessed data. One subject was excluded  
478 as no activation was found in one or more regions of interest. We also used global signal regression in our  
479 pre-processing pipeline. The time series for each ROI was computed as the first principal component of the  
480 voxel activity within a 6 mm sphere centred on the ROI coordinates (as listed in Table 4).

| <u>Region</u> | <u>MNI coordinates</u> |          |          | <u>Network</u> |
|---------------|------------------------|----------|----------|----------------|
|               | <i>x</i>               | <i>y</i> | <i>z</i> |                |
| PCC           | 0                      | -73      | 38       | DMN            |
| mPFC          | 0                      | 53       | 32       | DMN            |
| IAG           | -54                    | -61      | 29       | DMN            |
| rAG           | 57                     | -58      | 20       | DMN            |
| dACC          | 0                      | 17       | 41       | SN             |
| lAI           | -48                    | 14       | -7       | SN             |
| rAI           | 48                     | 14       | -7       | SN             |
| lFEF          | -30                    | -10      | 68       | DAN            |
| rFEF          | 30                     | -7       | 68       | DAN            |
| lIPS/SPL      | -42                    | -43      | 62       | DAN            |
| rIPS/SPL      | 39                     | -40      | 65       | DAN            |

481  
482 *Table 4 Coordinates of regions of interest. The DMN comprised of the posterior cingulate cortex (PCC),*  
483 *medial prefrontal cortex (mPFC), and left and right angular gyrus (IAG/rAG); the SN comprised of the dorsal*  
484 *anterior cingulate cortex (dACC), left and right anterior insula (lAI/rAI); and the DAN comprised the left*

485 and right frontal eye field (rFEF) and the left and right inferior parietal sulcus/superior parietal lobule  
486 (lIPS(SPL)/rIPS(SPL)).

487

488 *Anticorrelation Functional Connectivity Validation*

489 The functional connectivity matrix between regions of the DMN, SN, and DAN in the placebo condition  
490 was computed for all subjects. Since our arguments rest on the premise of functional anticorrelation  
491 between the resting-state networks (and similar second-order features are used for model estimation by the  
492 following spectral DCM analysis), 4 subjects that did not show evidence of the anticorrelation in the placebo  
493 condition were excluded from further analysis. As such, 20 subjects were left available for the following  
494 DCM analysis.

495

496 *Specification and Inversion of DCM*

497 A fully-connected DCM was specified using the 11 ROIs defined in Table 4, without any exogenous inputs.  
498 The DCM for each subject was then inverted using spectral DCM (Karl J. Friston et al., 2014; Razi, Kahan,  
499 Rees, & Friston, 2015) to infer the effective connectivity that best explains the observed cross-spectral  
500 density for each subject. This procedure was repeated for each of the three testing conditions. The DCM  
501 fitted the data very well and explained variance was over 85% across all subjects, and averaged 91%.

502

503 *Second Level Analysis Using Parametric Empirical Bayes*

504 The effective connectivity inferred by spectral DCM for each subject are taken to the second (group) level  
505 to test hypotheses about between-subject effects. A General Linear Model (GLM) is employed to  
506 decompose individual differences in effective connectivity into hypothesised group-average connection  
507 strengths plus unexplained noise. Hypotheses on the group-level parameters are tested within the Parametric  
508 Empirical Bayes (PEB) framework (K. J. Friston et al., 2016), where both the expected values and the  
509 covariance of the parameters are taken into account. That is, precise parameter estimates influence the

510 group-level result more strongly than uncertain estimates, which are down-weighted. Bayesian model  
511 reduction (BMR) is used as an efficient form of Bayesian model selection (K. J. Friston et al., 2016).

512

513 *Network Level Effective Connectivity and Hierarchical Organization*

514 The expected network-level connectivity was computed as the sum of the expected effective connectivity  
515 values between the corresponding ROIs. Then, following Zhou et. al., 2018 (Zhou et al., 2018) the  
516 hierarchical connectivity strength of each network was obtained by computing the difference between its  
517 averaged efferent and afferent connections (i.e., absolute values, see Supplementary S4). A similar  
518 approach was used for analysing hierarchical projections in the monkey brain (Goulas, Uylings, & Stiers,  
519 2012) and prefrontal cortex hierarchical organization in humans (Nee & D'Esposito, 2016; Zhou et al.,  
520 2018).

521

522 *References*

- 523 Andrews-Hanna, J. R., Reidler, J. S., Sepulcre, J., Poulin, R., & Buckner, R. L. (2010). Functional-  
524 anatomic fractionation of the brain's default network. *Neuron*, 65(4), 550-562.  
525 doi:10.1016/j.neuron.2010.02.005
- 526 Andrews-Hanna, J. R., Smallwood, J., & Spreng, R. N. (2014). The default network and self-  
527 generated thought: component processes, dynamic control, and clinical relevance.  
528 *Annals of the New York Academy of Sciences*, 1316(1), 29-52. doi:10.1111/nyas.12360
- 529 Averbeck, B. B., & Seo, M. (2008). The Statistical Neuroanatomy of Frontal Networks in the  
530 Macaque. *PLOS Computational Biology*, 4(4), e1000050.  
531 doi:10.1371/journal.pcbi.1000050
- 532 Batchelor, S. (2008). *Buddhism without beliefs : a contemporary guide to awakening*. London:  
533 Bloomsbury.
- 534 Blanke, O., & Metzinger, T. (2009). Full-body illusions and minimal phenomenal selfhood.  
535 *Trends Cogn Sci*, 13(1), 7-13. doi:10.1016/j.tics.2008.10.003
- 536 Bolton, T., Wotruba, D., Buechler, R., Theodoridou, A., Michels, L., Kollias, S., . . . Van De Ville, D.  
537 (2020). Triple Network Model Dynamically Revisited: Lower Salience Network State  
538 Switching in Pre-psychosis. *Frontiers in Physiology*, 11. doi:10.3389/fphys.2020.00066
- 539 Bonnelle, V., Ham, T. E., Leech, R., Kinnunen, K. M., Mehta, M. A., Greenwood, R. J., & Sharp, D.  
540 J. (2012). Salience network integrity predicts default mode network function after  
541 traumatic brain injury. *Proc Natl Acad Sci U S A*, 109(12), 4690-4695.  
542 doi:10.1073/pnas.1113455109

- 543 Bréchet, L., Grivaz, P., Gauthier, B., & Blanke, O. (2018). Common Recruitment of Angular Gyrus  
544 in Episodic Autobiographical Memory and Bodily Self-Consciousness. *Frontiers in*  
545 *Behavioral Neuroscience*, 12(270). doi:10.3389/fnbeh.2018.00270
- 546 Brewer, J. A., Garrison, K. A., & Whitfield-Gabrieli, S. (2013). What about the "Self" is Processed  
547 in the Posterior Cingulate Cortex? *Front Hum Neurosci*, 7, 647.  
548 doi:10.3389/fnhum.2013.00647
- 549 Brewer, J. A., Worhunsky, P. D., Gray, J. R., Tang, Y.-Y., Weber, J., & Kober, H. (2011). Meditation  
550 experience is associated with differences in default mode network activity and  
551 connectivity. *Proceedings of the National Academy of Sciences*, 108(50), 20254-20259.  
552 doi:10.1073/pnas.1112029108
- 553 Carhart-Harris, R. L. (2018). How do psychedelics work? *Current Opinion in Psychiatry*, 1.  
554 doi:10.1097/YCO.0000000000000467
- 555 Carhart-Harris, R. L., Bolstridge, M., Day, C. M. J., Rucker, J., Watts, R., Erritzoe, D. E., . . . Nutt,  
556 D. J. (2018). Psilocybin with psychological support for treatment-resistant depression:  
557 six-month follow-up. *Psychopharmacology*, 235(2), 399-408. doi:10.1007/s00213-017-  
558 4771-x
- 559 Carhart-Harris, R. L., & Friston, K. J. (2010). The default-mode, ego-functions and free-energy: a  
560 neurobiological account of Freudian ideas. *Brain*, 133(Pt 4), 1265-1283.  
561 doi:10.1093/brain/awq010
- 562 Carhart-Harris, R. L., & Friston, K. J. (2019). REBUS and the Anarchic Brain: Toward a Unified  
563 Model of the Brain Action of Psychedelics. *Pharmacological Reviews*, 71(3), 316-344.  
564 doi:10.1124/pr.118.017160
- 565 Carhart-Harris, R. L., Leech, R., Erritzoe, D., Williams, T. M., Stone, J. M., Evans, J., . . . Nutt, D. J.  
566 (2012). Functional Connectivity Measures After Psilocybin Inform a Novel Hypothesis of  
567 Early Psychosis. *Schizophrenia Bulletin*, 39(6), 1343-1351. doi:10.1093/schbul/sbs117
- 568 Carlos Bouso, J., Palhano-Fontes, F., Rodriguez-Fornells, A., Ribeiro, S., Sanches, R., Crippa, J. A.  
569 S., . . . Riba, J. (2015). Long-term use of psychedelic drugs is associated with differences  
570 in brain structure and personality in humans. *European Neuropsychopharmacology*,  
571 25(4), 483-492. doi:10.1016/j.euroneuro.2015.01.008
- 572 Chaminade, T., & Decety, J. (2002). Leader or follower? Involvement of the inferior parietal  
573 lobule in agency. *Neuroreport*, 13(15), 1975-1978. doi:10.1097/00001756-200210280-  
574 00029
- 575 Chand, G. B., Wu, J., Hajjar, I., & Qiu, D. (2017). Interactions of the Salience Network and Its  
576 Subsystems with the Default-Mode and the Central-Executive Networks in Normal Aging  
577 and Mild Cognitive Impairment. *Brain Connectivity*, 7(7), 401-412.  
578 doi:10.1089/brain.2017.0509
- 579 Chen, J. E., Glover, G. H., Greicius, M. D., & Chang, C. (2017). Dissociated patterns of anti-  
580 correlations with dorsal and ventral default-mode networks at rest. *Human Brain*  
581 *Mapping*, 38(5), 2454-2465. doi:<https://doi.org/10.1002/hbm.23532>
- 582 Chong, J. S. X., Ng, G. J. P., Lee, S. C., & Zhou, J. (2017). Salience network connectivity in the  
583 insula is associated with individual differences in interoceptive accuracy. *Brain Structure*  
584 *and Function*, 222(4), 1635-1644. doi:10.1007/s00429-016-1297-7
- 585 Cieri, F., & Esposito, R. (2019). Psychoanalysis and Neuroscience: The Bridge Between Mind and  
586 Brain. *Frontiers in Psychology*, 10(1983). doi:10.3389/fpsyg.2019.01983

- 587 Clark, A. (2013). Whatever next? Predictive brains, situated agents, and the future of cognitive  
588 science. *Behav Brain Sci*, 36(3), 181-204. doi:10.1017/s0140525x12000477
- 589 Connolly, P. (2018). Expected Free Energy Formalizes Conflict Underlying Defense in Freudian  
590 Psychoanalysis. *Front Psychol*, 9, 1264. doi:10.3389/fpsyg.2018.01264
- 591 Corbetta, M., & Shulman, G. (2002). Control of Goal-Directed and Stimulus-Driven Attention in  
592 the Brain. *Nature reviews. Neuroscience*, 3, 201-215. doi:10.1038/nrn755
- 593 Dambrun, M. (2017). Self-centeredness and selflessness: happiness correlates and mediating  
594 psychological processes. *PeerJ*, 5, e3306. doi:10.7717/peerj.3306
- 595 Di, X., & Biswal, B. B. (2014). Identifying the default mode network structure using dynamic  
596 causal modeling on resting-state functional magnetic resonance imaging. *NeuroImage*,  
597 86, 53-59. doi:<https://doi.org/10.1016/j.neuroimage.2013.07.071>
- 598 Dittrich, A. (1998). The standardized psychometric assessment of altered states of  
599 consciousness (ASCs) in humans. *Pharmacopsychiatry*, 31 Suppl 2, 80-84. doi:10.1055/s-  
600 2007-979351
- 601 Dixon, M. L., Andrews-Hanna, J. R., Spreng, R. N., Irving, Z. C., Mills, C., Girn, M., & Christoff, K.  
602 (2017). Interactions between the default network and dorsal attention network vary  
603 across default subsystems, time, and cognitive states. *NeuroImage*, 147, 632-649.  
604 doi:10.1016/j.neuroimage.2016.12.073
- 605 Doll, A., Hölzel, B. K., Boucard, C. C., Wohlschläger, A. M., & Sorg, C. (2015). Mindfulness is  
606 associated with intrinsic functional connectivity between default mode and salience  
607 networks. *Frontiers in Human Neuroscience*, 9, 461. doi:10.3389/fnhum.2015.00461
- 608 Egner, T., Monti, J. M. P., Tritschuh, E. H., Wieneke, C. A., Hirsch, J., & Mesulam, M. M. (2008).  
609 Neural Integration of Top-Down Spatial and Feature-Based Information in Visual Search.  
610 *The Journal of Neuroscience*, 28(24), 6141. doi:10.1523/JNEUROSCI.1262-08.2008
- 611 Etkin, A., Egner, T., & Kalisch, R. (2011). Emotional processing in anterior cingulate and medial  
612 prefrontal cortex. *Trends in Cognitive Sciences*, 15(2), 85-93.  
613 doi:10.1016/j.tics.2010.11.004
- 614 Fecteau, J. H., & Munoz, D. P. (2006). Salience, relevance, and firing: a priority map for target  
615 selection. *Trends Cogn Sci*, 10(8), 382-390. doi:10.1016/j.tics.2006.06.011
- 616 Fox, M. D., Corbetta, M., Snyder, A. Z., Vincent, J. L., & Raichle, M. E. (2006). Spontaneous  
617 neuronal activity distinguishes human dorsal and ventral attention systems. *Proceedings  
618 of the National Academy of Sciences*, 103(26), 10046-10051.  
619 doi:10.1073/pnas.0604187103
- 620 Fox, M. D., & Raichle, M. E. (2007). Spontaneous fluctuations in brain activity observed with  
621 functional magnetic resonance imaging. *Nature Reviews Neuroscience*, 8(9), 700-711.  
622 doi:10.1038/nrn2201
- 623 Fox, M. D., Snyder, A. Z., Vincent, J. L., Corbetta, M., Van Essen, D. C., & Raichle, M. E. (2005).  
624 The human brain is intrinsically organized into dynamic, anticorrelated functional  
625 networks. *Proceedings of the National Academy of Sciences of the United States of  
626 America*, 102(27), 9673. doi:10.1073/pnas.0504136102
- 627 Fox, M. D., Zhang, D., Snyder, A. Z., & Raichle, M. E. (2009). The global signal and observed  
628 anticorrelated resting state brain networks. *J Neurophysiol*, 101(6), 3270-3283.  
629 doi:10.1152/jn.90777.2008

- 630 Fransson, P. (2005). Spontaneous low-frequency BOLD signal fluctuations: an fMRI investigation  
631 of the resting-state default mode of brain function hypothesis. *Hum Brain Mapp*, 26(1),  
632 15-29. doi:10.1002/hbm.20113
- 633 Freud, S. (1894). *The neuro-psychoses of defence* (Vol. 1). London: Hogarth Press.
- 634 Friston, K. (2009). The free-energy principle: a rough guide to the brain? *Trends in Cognitive  
635 Sciences*, 13(7), 293-301. doi:<https://doi.org/10.1016/j.tics.2009.04.005>
- 636 Friston, K. (2010). The free-energy principle: a unified brain theory? *Nature Reviews  
637 Neuroscience*, 11, 127. doi:10.1038/nrn2787  
<https://www.nature.com/articles/nrn2787#supplementary-information>
- 638 Friston, K., Kilner, J., & Harrison, L. (2006). A free energy principle for the brain. *J Physiol Paris*,  
639 100(1-3), 70-87. doi:10.1016/j.jphysparis.2006.10.001
- 640 Friston, K. J. (2011). Functional and effective connectivity: a review. *Brain Connect*, 1(1), 13-36.  
641 doi:10.1089/brain.2011.0008
- 642 Friston, K. J., Harrison, L., & Penny, W. (2003). Dynamic causal modelling. *NeuroImage*, 19(4),  
643 1273-1302. doi:10.1016/s1053-8119(03)00202-7
- 644 Friston, K. J., Kahan, J., Biswal, B., & Razi, A. (2014). A DCM for resting state fMRI. *NeuroImage*,  
645 94, 396-407. doi:<https://doi.org/10.1016/j.neuroimage.2013.12.009>
- 646 Friston, K. J., Litvak, V., Oswal, A., Razi, A., Stephan, K. E., van Wijk, B. C. M., . . . Zeidman, P.  
647 (2016). Bayesian model reduction and empirical Bayes for group (DCM) studies.  
648 *NeuroImage*, 128, 413-431. doi:10.1016/j.neuroimage.2015.11.015
- 649 Goulas, A., Uylings, H. B. M., & Stiers, P. (2012). Mapping the Hierarchical Layout of the  
650 Structural Network of the Macaque Prefrontal Cortex. *Cerebral Cortex*, 24(5), 1178-  
651 1194. doi:10.1093/cercor/bhs399
- 652 Goyal, M., Singh, S., Sibinga, E. M., Gould, N. F., Rowland-Seymour, A., Sharma, R., . . .  
653 Haythornthwaite, J. A. (2014). Meditation programs for psychological stress and well-  
654 being: a systematic review and meta-analysis. *JAMA Intern Med*, 174(3), 357-368.  
655 doi:10.1001/jamainternmed.2013.13018
- 656 Greicius, M. D., & Menon, V. (2004). Default-Mode Activity during a Passive Sensory Task:  
657 Uncoupled from Deactivation but Impacting Activation. *J Cogn Neurosci*, 16(9), 1484-  
658 1492. doi:10.1162/0898929042568532
- 659 Griffiths, R. R., Johnson, M. W., Carducci, M. A., Umbricht, A., Richards, W. A., Richards, B. D., . . .  
660 Klinedinst, M. A. (2016). Psilocybin produces substantial and sustained decreases in  
661 depression and anxiety in patients with life-threatening cancer: A randomized double-  
662 blind trial. *Journal of Psychopharmacology*, 30(12), 1181-1197.  
663 doi:10.1177/0269881116675513
- 664 Grof, S. (1980). *LSD Psychotherapy*. Alameda, CA: Hunter House Publishers.
- 665 Ham, T. E., Bonnelle, V., Hellyer, P., Jilka, S., Robertson, I. H., Leech, R., & Sharp, D. J. (2014).  
666 The neural basis of impaired self-awareness after traumatic brain injury. *Brain : a journal  
667 of neurology*, 137(Pt 2), 586-597. doi:10.1093/brain/awt350
- 668 Hasenkamp, W., Wilson-Mendenhall, C. D., Duncan, E., & Barsalou, L. W. (2012). Mind  
669 wandering and attention during focused meditation: a fine-grained temporal analysis of  
670 fluctuating cognitive states. *NeuroImage*, 59(1), 750-760.  
671 doi:10.1016/j.neuroimage.2011.07.008
- 672

- 673 Herzog, R., Mediano, P. A. M., Rosas, F. E., Carhart-Harris, R., Perl, Y. S., Tagliazucchi, E., &  
674 Cofre, R. (2020). A mechanistic model of the neural entropy increase elicited by  
675 psychedelic drugs. *Scientific Reports*, 10(1), 17725. doi:10.1038/s41598-020-74060-6
- 676 Ho, J. T., Preller, K. H., & Lenggenhager, B. (2020). Neuropharmacological modulation of the  
677 aberrant bodily self through psychedelics. *Neurosci Biobehav Rev*, 108, 526-541.  
678 doi:10.1016/j.neubiorev.2019.12.006
- 679 Ide, J. S., Shenoy, P., Yu, A. J., & Li, C. S. (2013). Bayesian prediction and evaluation in the  
680 anterior cingulate cortex. *The Journal of Neuroscience*, 33(5), 2039-2047.  
681 doi:10.1523/jneurosci.2201-12.2013
- 682 Johnson, M., Richards, W., & Griffiths, R. (2008). Human hallucinogen research: guidelines for  
683 safety. In (Vol. 22, pp. 603-620). London, England.
- 684 Josipovic, Z., Dinstein, I., Weber, J., & Heeger, D. (2012). Influence of meditation on anti-  
685 correlated networks in the brain. *Frontiers in Human Neuroscience*, 5, 183. Retrieved  
686 from <https://www.frontiersin.org/article/10.3389/fnhum.2011.00183>  
<https://www.ncbi.nlm.nih.gov/pmc/articles/PMC3250078/pdf/fnhum-05-00183.pdf>
- 687 Lebedev, A. V., Lövdén, M., Rosenthal, G., Feilding, A., Nutt, D. J., & Carhart-Harris, R. L. (2015).  
688 Finding the self by losing the self: Neural correlates of ego-dissolution under psilocybin.  
689 *Human Brain Mapping*, 36(8), 3137-3153. doi:10.1002/hbm.22833
- 690 Legrand, D., & Ruby, P. (2009). What is self-specific? Theoretical investigation and critical  
691 review of neuroimaging results [American Psychological Association  
692 doi:10.1037/a0014172]. Retrieved
- 693 Leptourgos, P., Fortier-Davy, M., Carhart-Harris, R., Corlett, P., Dupuis, D., Halberstadt, A., . . .  
694 Jardri, R. (2020). Hallucinations Under Psychedelics and in the Schizophrenia Spectrum:  
695 An Interdisciplinary and Multiscale Comparison. *Schizophrenia Bulletin*.  
696 doi:10.1093/schbul/sbaa117
- 697 Liang, X., He, Y., Salmeron, B. J., Gu, H., Stein, E. A., & Yang, Y. (2015). Interactions between the  
698 salience and default-mode networks are disrupted in cocaine addiction. *The Journal of  
699 neuroscience : the official journal of the Society for Neuroscience*, 35(21), 8081-8090.  
700 doi:10.1523/JNEUROSCI.3188-14.2015
- 701 Manoliu, A., Riedl, V., Zherdin, A., Mühlau, M., Schwerthöffer, D., Scherr, M., . . . Sorg, C. (2014).  
702 Aberrant dependence of default mode/central executive network interactions on  
703 anterior insular salience network activity in schizophrenia. *Schizophr Bull*, 40(2), 428-  
704 437. doi:10.1093/schbul/sbt037
- 705 Menon, V. (2011). Large-scale brain networks and psychopathology: a unifying triple network  
706 model. *Trends Cogn Sci*, 15(10), 483-506. doi:10.1016/j.tics.2011.08.003
- 707 Menon, V. (2015). *Salience Network* (Vol. 2): Elsevier.
- 708 Menon, V. (2018). The Triple Network Model, Insight, and Large-Scale Brain Organization in  
709 Autism. *Biological Psychiatry*, 84(4), 236-238. doi:10.1016/j.biopsych.2018.06.012
- 710 Menon, V., & Uddin, L. Q. (2010). Saliency, switching, attention and control: a network model of  
711 insula function. *Brain structure & function*, 214(5-6), 655-667. doi:10.1007/s00429-010-  
712 0262-0
- 713 Metzinger, T. (2003). *Being no one: The self-model theory of subjectivity*. Cambridge, MA, US:  
714 MIT Press.

- 716 Millière, R. (2017). Looking for the Self: Phenomenology, Neurophysiology and Philosophical  
717 Significance of Drug-induced Ego Dissolution. *Frontiers in Human Neuroscience*, 11(245).  
718 doi:10.3389/fnhum.2017.00245
- 719 Millière, R., Carhart-Harris, R. L., Roseman, L., Trautwein, F.-M., & Berkovich-Ohana, A. (2018).  
720 Psychedelics, Meditation, and Self-Consciousness. *Frontiers in Psychology*, 9(1475).  
721 doi:10.3389/fpsyg.2018.01475
- 722 Müller, F., Dolder, P. C., Schmidt, A., Liechti, M. E., & Borgwardt, S. (2018). Altered network hub  
723 connectivity after acute LSD administration. *NeuroImage. Clinical*, 18, 694-701.  
724 doi:10.1016/j.nicl.2018.03.005
- 725 Nee, D. E., & D'Esposito, M. (2016). The hierarchical organization of the lateral prefrontal  
726 cortex. *eLife*, 5. doi:10.7554/eLife.12112
- 727 Northoff, G., Heinzel, A., de Greck, M., Bermpohl, F., Dobrowolny, H., & Panksepp, J. (2006).  
728 Self-referential processing in our brain--a meta-analysis of imaging studies on the self.  
729 *NeuroImage*, 31(1), 440-457. doi:10.1016/j.neuroimage.2005.12.002
- 730 Nour, M. M., & Carhart-Harris, R. L. (2017). Psychedelics and the science of self-experience. *Br J  
731 Psychiatry*, 210(3), 177-179. doi:10.1192/bjp.bp.116.194738
- 732 Nour, M. M., Evans, L., Nutt, D., & Carhart-Harris, R. L. (2016). Ego-Dissolution and Psychedelics:  
733 Validation of the Ego-Dissolution Inventory (EDI). *Frontiers in Human Neuroscience*, 10.  
734 doi:10.3389/fnhum.2016.00269
- 735 Nutt, D., & Carhart-Harris, R. (2020). The Current Status of Psychedelics in Psychiatry. *JAMA  
736 Psychiatry*. doi:10.1001/jamapsychiatry.2020.2171
- 737 Palaniyappan, L., & Liddle, P. F. (2012). Does the salience network play a cardinal role in  
738 psychosis? An emerging hypothesis of insular dysfunction. *J Psychiatry Neurosci*, 37(1),  
739 17-27. doi:10.1503/jpn.100176
- 740 Palhano-Fontes, F., Andrade, K. C., Tofoli, L. F., Santos, A. C., Crippa, J. A., Hallak, J. E., . . . de  
741 Araujo, D. B. (2015). The psychedelic state induced by ayahuasca modulates the activity  
742 and connectivity of the default mode network. *Plos One*, 10(2), e0118143.  
743 doi:10.1371/journal.pone.0118143
- 744 Peterson, A., Thome, J., Frewen, P., & Lanius, R. A. (2014). Resting-State Neuroimaging Studies:  
745 A New Way of Identifying Differences and Similarities among the Anxiety Disorders? *The  
746 Canadian Journal of Psychiatry*, 59(6), 294-300. doi:10.1177/070674371405900602
- 747 Preller, K. H., Burt, J. B., Ji, J. L., Schleifer, C. H., Adkinson, B. D., Stämpfli, P., . . . Anticevic, A.  
748 (2018). Changes in global and thalamic brain connectivity in LSD-induced altered states  
749 of consciousness are attributable to the 5-HT2A receptor. *eLife*, 7, e35082.  
750 doi:10.7554/eLife.35082
- 751 Preller, K. H., Herdener, M., Pokorny, T., Planzer, A., Kraehenmann, R., Stampfli, P., . . .  
752 Vollenweider, F. X. (2017). The Fabric of Meaning and Subjective Effects in LSD-Induced  
753 States Depend on Serotonin 2A Receptor Activation. *Curr Biol*, 27(3), 451-457.  
754 doi:10.1016/j.cub.2016.12.030
- 755 Preller, K. H., Pokorny, T., Hock, A., Kraehenmann, R., Stampfli, P., Seifritz, E., . . . Vollenweider,  
756 F. X. (2016). Effects of serotonin 2A/1A receptor stimulation on social exclusion  
757 processing. *Proc Natl Acad Sci U S A*, 113(18), 5119-5124. doi:10.1073/pnas.1524187113
- 758 Preller, K. H., Pokorny, T., Kraehenmann, R., Scheidegger, M., Dziobek, I., Staempfli, P., &  
759 Vollenweider, F. X. (2015). The 5-HT2A/1A agonist psilocybin reduces social pain and

- enhances empathy in healthy volunteers. *European Neuropsychopharmacology*, 25, S301-S301. doi:10.1016/s0924-977x(15)30364-3
- Preller, K. H., Razi, A., Zeidman, P., Stämpfli, P., Friston, K. J., & Vollenweider, F. X. (2019). Effective connectivity changes in LSD-induced altered states of consciousness in humans. *Proceedings of the National Academy of Sciences*, 116(7), 2743-2748. doi:10.1073/pnas.1815129116
- Preller, K. H., & Vollenweider, F. X. (2018). Phenomenology, Structure, and Dynamic of Psychedelic States. *Curr Top Behav Neurosci*, 36, 221-256. doi:10.1007/7854\_2016\_459
- Putcha, D., Ross, R. S., Cronin-Golomb, A., Janes, A. C., & Stern, C. E. (2016). Salience and Default Mode Network Coupling Predicts Cognition in Aging and Parkinson's Disease. *Journal of the International Neuropsychological Society : JINS*, 22(2), 205-215. doi:10.1017/S1355617715000892
- Raichle, M. E. (2015). The brain's default mode network. *Annu Rev Neurosci*, 38, 433-447. doi:10.1146/annurev-neuro-071013-014030
- Raichle, M. E., MacLeod, A. M., Snyder, A. Z., Powers, W. J., Gusnard, D. A., & Shulman, G. L. (2001). A default mode of brain function. *Proc Natl Acad Sci U S A*, 98(2), 676-682. doi:10.1073/pnas.98.2.676
- Ramirez Barrantes, R., Arancibia, M., Stojanova, J., Aspé-Sánchez, M., Córdova, C., & Henríquez, R. A. (2019). Default Mode Network, Meditation, and Age-Associated Brain Changes: What Can We Learn from the Impact of Mental Training on Well-Being as a Psychotherapeutic Approach? *Neural Plasticity*, 2019, 1-15. doi:10.1155/2019/7067592
- Razi, A., Kahan, J., Rees, G., & Friston, K. J. (2015). Construct validation of a DCM for resting state fMRI. *NeuroImage*, 106, 1-14. doi:<https://doi.org/10.1016/j.neuroimage.2014.11.027>
- Roseman, L., Nutt, D. J., & Carhart-Harris, R. L. (2018). Quality of Acute Psychedelic Experience Predicts Therapeutic Efficacy of Psilocybin for Treatment-Resistant Depression. *Frontiers in Pharmacology*, 8, 974. doi:10.3389/fphar.2017.00974
- Ross, S., Bossis, A., Guss, J., Agin-Liebes, G., Malone, T., Cohen, B., . . . Schmidt, B. L. (2016). Rapid and sustained symptom reduction following psilocybin treatment for anxiety and depression in patients with life-threatening cancer: a randomized controlled trial. *Journal of Psychopharmacology*, 30(12), 1165-1180. doi:10.1177/0269881116675512
- Ruban, A., & Kolodziej, A. A. (2018). Changes in default-mode network activity and functional connectivity as an indicator of psychedelic-assisted psychotherapy effectiveness. *Neuropsychiatra I Neuropsychologia*, 13(3), 91-97. doi:10.5114/nan.2018.81249
- Safron, A. (2020, November 30). On the Varieties of Conscious Experiences: Altered Beliefs Under Psychedelics (ALBUS). <https://doi.org/10.31234/osf.io/zqh4b>
- Scalabrini, A., Vai, B., Poletti, S., Damiani, S., Mucci, C., Colombo, C., . . . Northoff, G. (2020). All roads lead to the default-mode network-global source of DMN abnormalities in major depressive disorder. *Neuropsychopharmacology*, 45(12), 2058-2069. doi:10.1038/s41386-020-0785-x
- Seeley, W. W., Menon, V., Schatzberg, A. F., Keller, J., Glover, G. H., Kenna, H., . . . Greicius, M. D. (2007). Dissociable intrinsic connectivity networks for salience processing and executive control. *The Journal of Neuroscience*, 27(9), 2349-2356. doi:10.1523/jneurosci.5587-06.2007

- 804 Sridharan, D., Levitin, D. J., & Menon, V. (2008). A critical role for the right fronto-insular cortex  
805 in switching between central-executive and default-mode networks. *Proceedings of the  
806 National Academy of Sciences*, 105(34), 12569. doi:10.1073/pnas.0800005105
- 807 Stoliker, D., Egan, G., Friston, K., & Razi, A. (2021). Neural Mechanisms and Psychology of  
808 Psychedelic Ego Dissolution. In: PsyArXiv.
- 809 Stoliker, D., Egan, G., & Razi, A. (2021). Reduced precision underwrites ego dissolution and  
810 therapeutic outcomes under psychedelics. In: PsyArXiv.
- 811 Studerus, E., Gamma, A., & Vollenweider, F. X. (2010). Psychometric evaluation of the altered  
812 states of consciousness rating scale (OAV). *Plos One*, 5(8), e12412-e12412.  
813 doi:10.1371/journal.pone.0012412
- 814 Swanson, L. R. (2018). Unifying Theories of Psychedelic Drug Effects. *Frontiers in Pharmacology*,  
815 9(172). doi:10.3389/fphar.2018.00172
- 816 Swick, D., Ashley, V., & Turken, U. (2011). Are the neural correlates of stopping and not going  
817 identical? Quantitative meta-analysis of two response inhibition tasks. *NeuroImage*,  
818 56(3), 1655-1665. doi:10.1016/j.neuroimage.2011.02.070
- 819 Szczepanski, S. M., Pinsky, M. A., Douglas, M. M., Kastner, S., & Saalmann, Y. B. (2013).  
820 Functional and structural architecture of the human dorsal frontoparietal attention  
821 network. *Proceedings of the National Academy of Sciences*, 110(39), 15806.  
822 doi:10.1073/pnas.1313903110
- 823 Thompson, K. G., Biscoe, K. L., & Sato, T. R. (2005). Neuronal basis of covert spatial attention in  
824 the frontal eye field. *The Journal of Neuroscience*, 25(41), 9479-9487.  
825 doi:10.1523/jneurosci.0741-05.2005
- 826 Uddin, L. Q., Kelly, A. M., Biswal, B. B., Castellanos, F. X., & Milham, M. P. (2009). Functional  
827 connectivity of default mode network components: correlation, anticorrelation, and  
828 causality. *Hum Brain Mapp*, 30(2), 625-637. doi:10.1002/hbm.20531
- 829 Uddin, L. Q., Molnar-Szakacs, I., Zaidel, E., & Iacoboni, M. (2006). rTMS to the right inferior  
830 parietal lobule disrupts self-other discrimination. *Social cognitive and affective  
831 neuroscience*, 1(1), 65-71. doi:10.1093/scan/nsl003
- 832 Vogt, B. A., & Pandya, D. N. (1987). Cingulate cortex of the rhesus monkey: II. Cortical afferents.  
833 *Journal of Comparative Neurology*, 262(2), 271-289.  
834 doi:<https://doi.org/10.1002/cne.902620208>
- 835 Vollenweider, F. X. (1998). Advances and pathophysiological models of hallucinogenic drug  
836 actions in humans: a preamble to schizophrenia research. *Pharmacopsychiatry*, 31 Suppl  
837 2, 92-103. doi:10.1055/s-2007-979353
- 838 Vollenweider, F. X., Leenders, K. L., Scharfetter, C., Maguire, P., Stadelmann, O., & Angst, J.  
839 (1997). Positron emission tomography and fluorodeoxyglucose studies of metabolic  
840 hyperfrontality and psychopathology in the psilocybin model of psychosis.  
841 *Neuropsychopharmacology*, 16(5), 357-372. doi:10.1016/s0893-133x(96)00246-1
- 842 Vollenweider, F. X., & Preller, K. H. (2020). Psychedelic drugs: neurobiology and potential for  
843 treatment of psychiatric disorders. *Nature Reviews Neuroscience*, 21(11), 611-624.  
844 doi:10.1038/s41583-020-0367-2
- 845 Wotruska, D., Michels, L., Buechler, R., Metzler, S., Theodoridou, A., Gerstenberg, M., . . .  
846 Heekeren, K. (2013). Aberrant Coupling Within and Across the Default Mode, Task-

- 847 Positive, and Salience Network in Subjects at Risk for Psychosis. *Schizophrenia Bulletin*,  
848 40. doi:10.1093/schbul/sbt161
- 849 Yaden, D. B., & Griffiths, R. R. (2020). The Subjective Effects of Psychedelics Are Necessary for  
850 Their Enduring Therapeutic Effects. *ACS Pharmacology & Translational Science*.  
851 doi:10.1021/acsptsci.0c00194
- 852 Yaoi, K., Osaka, M., & Osaka, N. (2015). Neural correlates of the self-reference effect: evidence  
853 from evaluation and recognition processes. *Frontiers in Human Neuroscience*, 9(383).  
854 doi:10.3389/fnhum.2015.00383
- 855 Zhou, Y., Friston, K. J., Zeidman, P., Chen, J., Li, S., & Razi, A. (2018). The Hierarchical  
856 Organization of the Default, Dorsal Attention and Salience Networks in Adolescents and  
857 Young Adults. *Cereb Cortex*, 28(2), 726-737. doi:10.1093/cercor/bhx307
- 858